INTERNATIONAL JOURNAL OF GEOMAGNETISM AND AERONOMY
VOL. 6, GI1005, doi:10.1029/2004GI000077, 2005

Expansion of solar corona in the Sun's gravitational field and formation of the heliospheric current sheet

I. M. Podgorny

Institute of Astronomy, Russian Academy of Sciences, Moscow, Russia

A. I. Podgorny

Lebedev Physical Institute, Russian Academy of Sciences, Moscow, Russia

Received 24 May 2004; revised 22 March 2005; accepted 3 May 2005; published 18 October 2005.

[1] Taking into account gravitation and the temperature gradient, three-dimensional MHD simulation of solar corona expansion in a dipole magnetic field was performed. Dissipation, compressibility, and anisotropy of thermal conductivity were taken into consideration. For calculations, the PERESVET code was used. It was been shown that a heliospheric current sheet having a normal component of magnetic field is formed. An important result is that the establishment of the stationary plasma outflow has been found to be extremely sensitive to the corona plasma parameters. For typical corona parameters, the flow becomes supersonic at a distance of more than three solar radii. *INDEX TERMS:* 7509 Solar Physics, Astrophysics, and Astronomy: Corona; 7827 Space Plasma Physics: Kinetic and MHD theory; 7524 Solar Physics, Astrophysics, and Astronomy: Magnetic fields; *KEYWORDS:* Solar corona; Heliospheric current sheet; Supersonic plasma outflow.

Citation: Podgorny, I. M., and A. I. Podgorny (2005), Expansion of solar corona in the Sun's gravitational field and formation of the heliospheric current sheet, *Int. J. Geomagn. Aeron., 6,* GI1005, doi:10.1029/2004GI000077.

1. Introduction

[2] To our knowledge, *Parker* [1963] was the first to consider the possibility of acceleration of the solar corona material against solar gravitation. He showed that it is possible to find such a constant of integration in the equation for plasma motion under the action of pressure gradient that acceleration is continuous and reaches the supersonic velocity at a critical distance from the Sun. The process was treated in the isothermal approximation; the effect of magnetic field was ignored. The isothermal conditions are unjustified, because temperature in the corona is ∼200 eV, and in the region of the Earth's orbit it is ∼20 eV. In our numerical experiment these limitations are absent. The consideration of the solar corona expansion involves taking into account thermal conductivity and therefore a nonzero temperature gradient.

[3] Spacecraft measurements have shown that the solar corona expansion leads to formation of a supersonic plasma flow (solar wind) and extension of the solar magnetic field lines. The configuration of the interplanetary field near the ecliptic plane is mainly determined by the current in the closed heliospheric current sheet. The current sheet separates the regions with the field lines directed toward the Sun and away from the Sun. The structure of the heliospheric current sheet was studied at crossings of the sheet by spacecrafts. However, it is impossible to reveal a complete picture of the magnetic field distribution inside the sheet from individual crossings [*Crooker et al.*, 2001; *Smith*, 2001]. The possibility of generation of current sheets in the corona was earlier reported by *Pneuman and Kopp* [1971], *Somov and Syrovatsky* [1971], and *Podgorny and Podgorny* [1995]. The interplanetary magnetic field in the vicinity of the current sheet was first considered in the two-dimensional geometry [*Pneuman and Kopp*, 1971; *Somov and Syrovatsky*, 1971]. In these papers, gravitation was neglected, which can be justified by a high thermal velocity of hydrogen ions in the corona, comparable with the cosmic velocity. However, the simplifying assumption of the existence of a neutral line above the arched magnetic lines is not correct. In the work of *Pneuman and Kopp* [1971], the plasma motion across the magnetic field was forbidden. With this condition, continuous evaporation from the Sun's surface would lead to an unlimited growth in the corona density in the regions with closed field lines if there is no plasma motion across the field lines. The main conclusions of these works on the ab-

1524–4423/05/2004GI000077$18.00

sence of the normal magnetic field component in the current sheet and existence of two types of magnetic lines (closed and open) are even more dubious. The neutral sheet cannot exist for a long time because of instability [see, e.g., *Laval et al.*, 1966]. The current sheet stability can be provided by the normal component and flow along the sheet [*Podgorny and Podgorny*, 1995], and therefore the heliospheric current sheet cannot be neutral. Some critical remarks on the formulation of the problem by *Pneuman and Kopp* [1971] were given by *Koutchmy and Livshits* [1992].

[4] The consideration of the steady state flow of magnetized plasma of the corona taking into account the Sun's rotation but assuming that the corona is isothermal was given by *Pisanko* [1985]. However, like in the works of *Pneuman and Kopp* [1971] and *Somov and Syrovatsky* [1971], the normal component of the magnetic field in the current sheet was assumed to be zero.

[5] The incorrectness of the conclusion on the absence of the normal magnetic field component in the heliospheric current sheet is obvious. Such a current cannot arise in a neutral ring stationary current sheet. To generate current in the sheet, the flow of a conducting material across the magnetic field must exist. In the MHD approximation, the Ohm's law has the form $j/\sigma = \mathbf{V} \times \mathbf{B}/c$. The polarization electric field $\mathbf{E} = -\mathbf{V} \times \mathbf{B}/c$ arises when a bounded conductor moves across the field, because in this case $j = 0$ and there are charges of opposite signs at the conductor ends. In the ring current formed at radial expansion of the solar corona, charges move unhindered under the action of the Lorentz force $e\mathbf{V} \times \mathbf{B}/c$, and no polarization arises. The Ohm's law in the case of the ring current acquires the form $j/\sigma = \mathbf{V} \times \mathbf{B}/c$. There are no other reasons for the ring current generation. It can be generated by the flow of a conducting material only in the case of the nonzero magnetic field component normal to the sheet B_n. Actually, in this case we have the MHD generator connected to a load with zero resistance. The current strength in this generator is determined by internal resistance. The presence of B_n means that division of the magnetic field lines into closed and open ones, as done by *Pneuman and Kopp* [1971], is incorrect. All the field lines emerging from a Sun's hemisphere enter the other hemisphere after crossing the current sheet.

[6] MHD simulation of the stationary solar wind in the solar magnetic field by *Usmanov* [1993] has shown that there is no reason to believe that the current sheet is neutral, and the data reported by *Usmanov* [1999] clearly indicate that the normal magnetic field component exists. However, *Usmanov* [1993, 1999] adopted several frequently used simplifications. In particular, thermal balance and temperature gradient in the expanding plasma were ignored. Three-dimensional numerical MHD simulation of the solar corona expansion in the dipole magnetic field of the Sun [*Minami et al.*, 2002; *Podgorny et al.*, 2004] taking into account dissipative processes and nonisothermality of plasma has revealed that the normal component of the magnetic field is an integral feature of the heliospheric current sheet. Below we present results of three-dimensional MHD simulation that demonstrate the role of gravitation in the corona expansion leading to formation of the current sheet. In the calculations, the rotation of the Sun that gives rise to the spiral structure of the interplanetary field is not taken into consideration. The spiral structure means that a radial component of the Lorentz force $B_z\omega r/c$ appears, and, in addition to the azimuthal current component j_φ, the sheet has a radial component j_r. Here, r is the distance to the Sun, and ω is the angular frequency of the Sun's rotation. The idea that the radial current component must exist in the equatorial plane was first advanced by *Alfvén* [1981], and the generation of this component was demonstrated by *Israelevich et al.* [2001].

2. Numerical Experiment

[7] A complete system of MHD equations was solved numerically by using a modified PERESVET code [*Podgorny and Podgorny*, 1996]. An absolutely implicit finite difference scheme conservative with respect to magnetic flux was used. It was solved by the iteration method. Owing to the use of the conservative scheme, the errors due to inaccuracy of approximation of div$\mathbf{B}$ by its finite difference analog could be avoided. The numerical method also included automatic multilevel division of the time step in the regions of large gradients of quantities. These capabilities of the scheme allowed stabilization of the majority of numerical instabilities. The code provided for graphical presentation of the magnetic field lines in the three-dimensional space. Anisotropy of thermal conductivity in the magnetic field, compressibility, and dissipative processes were taken into consideration. The dimensionless units of density ($\rho_0 = 10^4 m_i = 1.67 \times 10^{-20}$ g cm^{-3}), temperature ($T_0 = 20$ eV), magnetic field ($B_0 = 1$ G), velocity ($V_0 = B_0/\sqrt{4\pi\rho_0} \approx 2 \times 10^9$ cm s^{-1}), length ($L_0 = 8R_\odot \approx 6 \times 10^{11}$ cm), time ($t_0 = L_0/V_0 \sim 300$ s), and current density ($j_0 \sim 1.3 \times 10^{-12}$ A cm^{-2}) were used. Here, $m_i = 1.67 \times 10^{-24}$ is the mass of proton, and $R_\odot = 6.9 \times 10^{10}$ cm is the Sun's radius. The system of three-dimensional MHD equations in the dimensionless form is

$$\frac{\partial \mathbf{B}}{\partial t} = \mathrm{rot}(\mathbf{V} \times \mathbf{B}) - \frac{1}{Re_m}\mathrm{rot}\left(\frac{\sigma_0}{\sigma}\mathrm{rot}\mathbf{B}\right) \tag{1}$$

$$\frac{\partial \rho}{\partial t} = -\mathrm{div}(\mathbf{V}\rho) \tag{2}$$

$$\frac{\partial \mathbf{V}}{\partial t} = -(\mathbf{V}\nabla)\mathbf{V} - \frac{\beta_0}{2\rho}\nabla(\rho T) -$$

$$\frac{1}{\rho}(\mathbf{B} \times \mathrm{rot}\mathbf{B}) + \frac{1}{Re\rho}\Delta\mathbf{V} + G_g\mathbf{G} \tag{3}$$

$$\frac{\partial T}{\partial t} = -(\mathbf{V}\nabla)T - (\gamma - 1)T\mathrm{div}\mathbf{V} +$$

$$(\gamma - 1)\frac{2\sigma_0}{Re_m\sigma\beta_0\rho}(\mathrm{rot}\mathbf{B})^2 - (\gamma - 1)G_q\rho L'(T) +$$

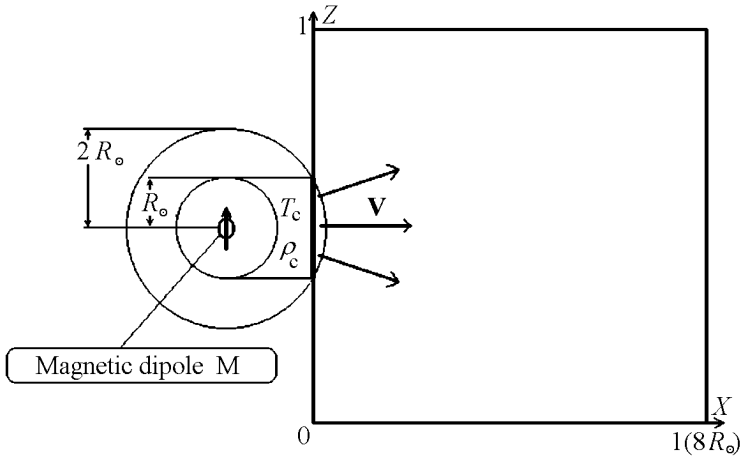

Figure 1. Scheme showing position of the Sun relative to the computational domain in the symmetry plane.

$$\frac{\gamma-1}{\rho}\mathrm{div}(\mathbf{e}_\parallel\kappa_{dl}(\mathbf{e}_\parallel,\nabla T)+\mathbf{e}_{\perp1}\kappa_{\perp dl}(\mathbf{e}_{\perp1},\nabla T)+$$

$$\mathbf{e}_{\perp2}\kappa_{\perp dl}(\mathbf{e}_{\perp1},\nabla T)) \quad (4)$$

[8] In equations (1)–(4), $Re_m = L_0V_0/\nu_{m0}$ is the magnetic Reynolds number, $\nu_{m0} = c^2/4\pi\sigma_0$ is the magnetic viscosity for conductivity σ at temperature T_0, and σ is the conductivity, $\sigma_0/\sigma = T^{-3/2}$. The dimensionless coefficient $\beta_0 = 8\pi n_0 kT_0/B_0^2$, where $n_0 = \rho_0/m_i$. It should be emphasized that β_0 in this form is not the ratio between plasma pressure and pressure of magnetic field at a definite point in space, it is simply a dimensionless coefficient expressed through the dimensionless units used for the calculations. The term including viscosity does not exert a considerable influence on the results; it is important for increasing the stability of the finite difference scheme. $Re = \rho_0L_0V_0/\eta$ is the Reynolds number, η is the viscosity, $G_q = L(T_0)\rho_0t_0/T_0$, $L(T_{\mathrm{dimens}})$ is the radiation function for ionization equilibrium in the corona, $T_{\mathrm{dimens}} = T_0T$. $L'(T) = L(T_{\mathrm{dimens}})/L(T_0)$ is the dimensionless radiation function. In the problem being solved, radiation did not have a strong effect; $\mathbf{e}_\parallel$, $\mathbf{e}_{\perp1}$, $\mathbf{e}_{\perp2}$ are the orthogonal unit vectors parallel and perpendicular to the magnetic field; $\kappa_{dl} = \kappa/(\Pi\kappa_0)$ is the dimensionless coefficient of thermal conductivity along the magnetic field; $\Pi = \rho_0L_0V_0/\kappa_0$ is the Peclet number; κ_0 is the thermal conductivity at temperature T_0; κ is the thermal conductivity; $\kappa/\kappa_0 = T^{5/2}$; $\kappa_{\perp dl} = [(\kappa\kappa_0^{-1}\Pi^{-1})(\kappa_B\kappa_{0B}^{-1}\Pi_B^{-1})]/[(\kappa\kappa_0^{-1}\Pi^{-1}) + (\kappa_B\kappa_{0B}^{-1}\Pi_B^{-1})]$ is the dimensionless coefficient of thermal conductivity in the direction perpendicular to the magnetic field; $\Pi_B = \rho_0L_0V_0/\kappa_{0B}$ is the Peclet number for the thermal conductivity across a strong magnetic field (when the cyclotron radius is much smaller than the free path). Thermal conductivity across a strong magnetic field is denoted as κ_B; and κ_{0B} is its magnitude for temperature T_0, plasma density ρ_0 and magnetic field B_0; $\kappa_B/\kappa_{0B} = \rho^2B^{-2}T^{-1/2}$. $G_g\mathbf{G}$ is the dimensionless gravitational acceleration. $G_g = t_0^2/L_0$, $\mathbf{G}$ is the gravitational acceleration, and γ is the adiabatic constant.

[9] The parameters used for calculations were: $\gamma = 5/3$, $Re_m = 8\times10^4$, $Re = 10^4$, $\beta_0 = 8\times10^{-6}$, $\Pi = 2$, $\Pi_B = 2\times10^6$. (We repeat here, that β_0 is not the ratio between plasma pressure and magnetic pressure at a definite point in space, it is only coefficient in equations (1)–(4), which is determined by dimensionless units of pressure and magnetic field). In numerical and laboratory simulation it is impossible to use very big and very little dimensionless parameters. These parameters are chosen bigger or less than unit, but not precisely by the same order of magnitude. The principles according to which the dimensionless parameters were chosen were described by *Podgorny and Podgorny* [1995, 1996]. For the numerical calculations, the grid $41\times41\times41$ was used; therefore the magnetic Reynolds number was ∼50.

[10] The computational domain was a cube with sides $8R_\odot$, in dimensionless units $0 \le x \le 1$, $0 \le y \le 1$, $0 \le z \le 1$. The positions of the Sun, corona, and computational domain in the $y = 0.5$ plane are shown in Figure 1. The dipole giving rise to the magnetic field $B_0 \approx 0.8$ G on the Sun's surface is parallel to the Z axis. The magnetic moment of the dipole in dimensionless units is $\mathbf{M}_1 = \{M_{1x} = 0, M_{1y} = 0, M_{1z} = 9.6\times10^{-2}\}$. Its center is at the point $\mathbf{R}_1 = \{x_1 = -0.217, y_1 = 0.5, z_1 = 0.5\}$. On the face $x = 0$, at the point $y = 0.5$ and $z = 0.5$, the magnetic field is 0.15 G. The lines of the initial (dipole) magnetic field are presented in Figure 2a.

[11] The vacuum medium cannot be described in the framework of the MHD approximation. For this reason, at $t = 0$ in the computational domain, an extremely low concentration of 10^{-1} cm^{-3}, whose influence on the dynamics of the corona plasma that expanded in the computational domain was negligibly small, was specified. At the initial moment of time, the temperature inside the region was taken to be as low as 20 eV.

[12] At $t = 0$, a thermal expansion of the corona began. The corona parameters ($\rho_c/m_i = 2\times10^7$ cm^{-3}, $T_c = 200$ eV) were specified on the face $x = 0$ in the circle formed by the intersection of this face and a spherical surface with the cen-

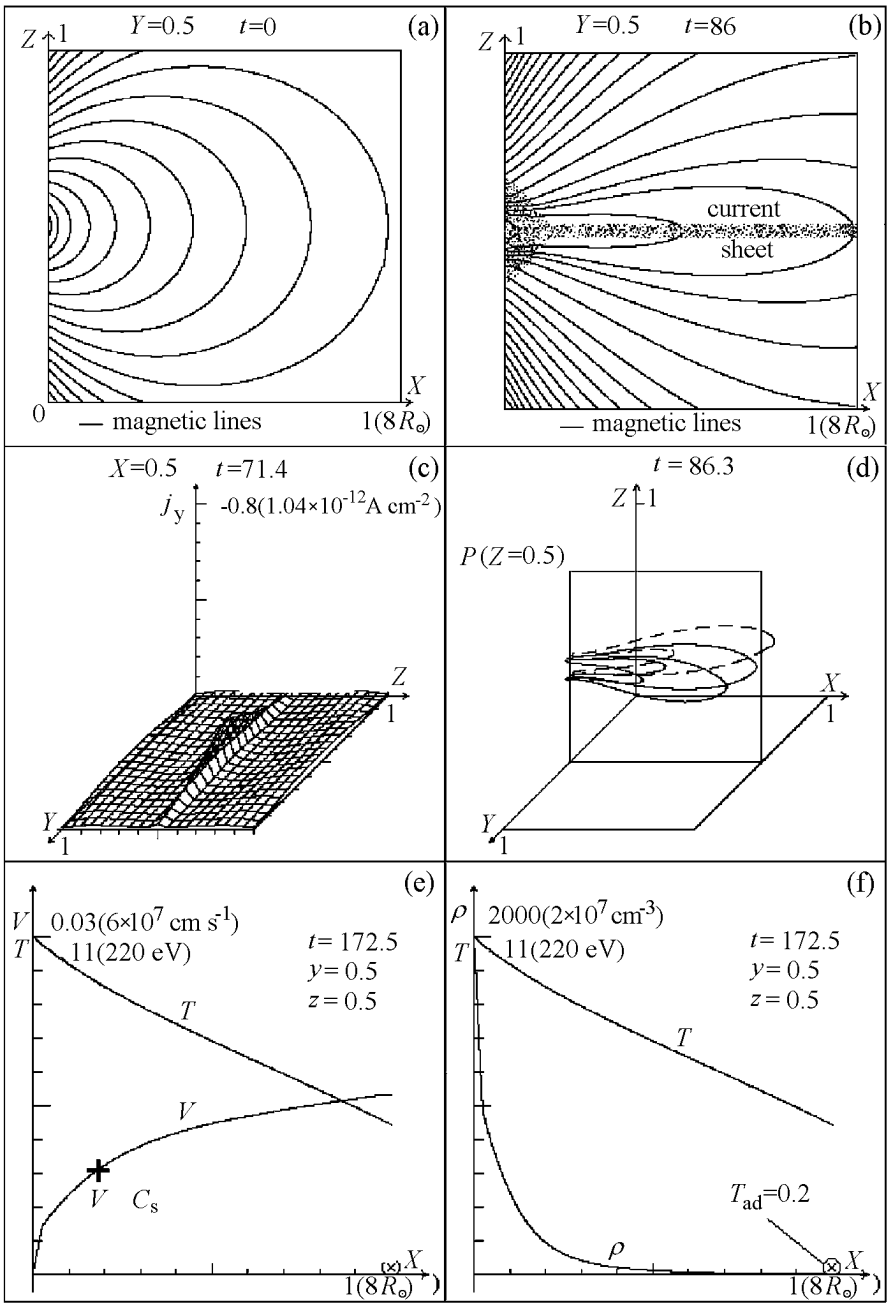

Figure 2. Results of calculations neglecting gravitation. (a) Dipole magnetic field lines; (b) field lines and position of the current sheet (crosshatched region); (c) current density distribution; (d) magnetic field lines in the three-dimensional space; and (e and f) radial distribution of plasma parameters.

ter (−0.217, 0.5, 0.5) and radius $2R_\odot$ (Figure 1). The center of the circle was ($y = 0.5$, $z = 0.5$), and its radius was 0.125. The velocity of plasma outflow from the corona was found from the continuity equation, so that the mass flow in the numerical experiment corresponded to the loss of the Sun's mass carried away by the solar wind ($\sim 10^{-14}$ of the Sun's mass per year). From this condition, the velocity of inflow into the region $V_x = 2.5 \times 10^{-4}$ was specified at the boundary $x = 0$ in the circle with the center ($y = 0.5$, $z = 0.5$) and radius 0.125. The self-consistent values of ρ, T, and V automatically established in the process of numerical solution of the MHD equations at thermal expansion of corona plasma. The current of the current sheet could freely flow in and out through the planes $y = 0$ and $y = 1$.

[13] It should be noted that, formally, the parameter β_0 did not correspond to the ratio between pressures at any point. At the point $x = 0$, $y = 0.5$, and $z = 0.5$ the β parameter is 8. In the vicinity of this point in the com-

putational domain, where the condition approximated the vacuum one, $\beta = 4 \times 10^{-9}$ at the initial moment.

[14] The most delicate problem in specifying the boundary conditions is setting the magnetic field at the rightmost boundary $X = 1$. In the process of calculations, and hence extension of field lines along the X axis, all components (B_x, B_y, B_z) undergo significant changes, and the tilt of the field line with respect to the $X = 1$ plane also changes. Therefore it is impossible to specify the magnetic field at the boundary $X = 1$. Setting $j = 0$ is also unacceptable because, in the process of extension of field lines, the current sheet reaches the right boundary. The best approximation is to assume $dj/dx = 0$. To be more certain that the obtained solution corresponds to the conditions in the solar wind, a layer boundary $X = 1$ which is by a factor of 2–3 thicker than the current sheet can be excluded from the consideration.

3. Corona Expansion: Gravitation Excluded

[15] The earlier published three-dimensional MHD calculations [*Minami et al.*, 2002; *Podgorny et al.*, 2004] without regard for gravitation ($G = 0$) showed that the heliospheric current sheet formed at deformation of the solar magnetic field by the corona plasma flow is not neutral. It has a nonzero normal component of the magnetic field. The configuration of the magnetic field and position of the current sheet (crosshatched region) are shown in Figure 2b. For comparison, Figure 2a presents the lines of the initial (dipole) field. In all the figures, the time and coordinates in the computational domain are given in dimensionless units, as in Figure 1. The distribution of current in the sheet in the $X =$const plane is depicted in Figure 2c. The values in Figure 2 are shown in dimensionless and dimensional (in brackets) units. The three-dimensional configuration of the magnetic field with the heliospheric current sheet is presented in Figure 2d. To facilitate spatial perception, a transparent virtual plane $P(Y = 0.5)$ is introduced. The magnetic field lines located in front of the plane and in the plane are shown by solid lines, and the field lines behind the plane are shown by dashed lines. All the field lines are extended along the X axis as compared with the dipole field lines.

[16] Figures 2e and 2f present distributions of the plasma velocity, temperature, and plasma density corresponding to the steady state regime. At a distance of ∼3.6 radii of the Sun from its center, the plasma velocity is 1.8×10^7 cm s^{-1}, i.e., it reaches the velocity of sound $C_s = (\gamma nkT/m_i)^{1/2}$. The point of transition to the supersonic flow is marked by a cross. The plasma temperature at a distance of ∼10 radii exceeds by more than an order of magnitude its value corresponding to the adiabatic cooling $T \sim \rho^{\gamma-1}$. The temperature corresponding to the adiabatic cooling is shown in Figure 2f by a circled cross. The temperature distribution in the plasma flow accelerated by the pressure gradient is governed by two basic factors, i.e., cooling at expansion and thermal conductivity. The role of radiation is negligibly small. Calculations have shown that the flow velocity at corona expansion is the highest in the region with nonzero density and temperature gradients. At first, the velocity maximum is in the computational domain. Then, when moving away from the Sun, the velocity maximum crosses the right boundary and goes beyond the domain.

4. Role of Gravitation

[17] The calculations in which real plasma parameters in the solar corona were specified and the gravitational forces of the Sun were taken into account have shown that, because of a high ∇P at the start of calculations, the effect of gravitation is nearly unnoticeable, and the distributions of plasma parameters at $t < 25$ turn out to be similar to those in the absence of gravitation (Figure 3). As the corona expands, the velocity maximum moves away from the Sun. The highest velocity is 5.5×10^7 cm s^{-1}. The maximum velocity of plasma flow is reached at the portion of the X axis where density and temperature gradients are not zero. However, as the corona expands and the gradients of the plasma density and temperature decrease, the force ∇P and gravitational force near the left boundary become comparable, and the flow velocity becomes lower than in the calculations assuming zero gravitation. A local decrease in velocity leads to a local plasma accumulation, i.e., to an increase in the density. As this takes place, the gradient near the left boundary $\nabla(nkT)/nM_i$ again increases, and the plasma velocity directed away from the Sun restores its value. This again causes smoothing of the gradient, i.e., the flow is no longer stable. This leads to the conclusion that an additional acceleration is needed for the stable generation of the solar wind in the presence of gravitation. Such an additional acceleration mechanism could be MHD waves generated on the photosphere and absorbed in the corona [*Chashey*, 1997].

[18] The nonstationarity of the flow in the vicinity of the Sun obtained in calculations allowing for gravitation can also be a result of an incorrect choice of the dimensionless parameter $\beta_0 = 8\pi n_0 kT_0/B_0^2$. It follows from the approximate Parker's formula that the solution is very sensitive to the integration constant, and the solar wind can be formed only under clearly defined conditions in the corona. By assuming that in the corona $kT = 200$ eV and $n = 2 \times 10^7$ cm^{-3}, we take into consideration only a pressure gradient of the electron gas. However, it can hardly be expected that the electron temperature of the corona considerably exceeds the ion temperature because the time during which the electron and proton temperatures become equal, estimated as $\tau(c) \sim 2 \times 10^7 T_e^{3/2}/n$, is not longer than an hour. Direct measurements of the electron temperature obtained from an ionization equilibrium and the ion temperature through Doppler broadening of spectral lines also point to $T_e \sim 200$ eV and $T_e \sim T_i$ [*Doschek and Feldman*, 2000; *Seely et al.*, 1997]. Here, T_e is the electron temperature in eV, and n is the number of electrons in cm^{-3}. If the electron temperature T_e in the corona plasma is comparable to the ion temperature T_i, the dimensionless parameter of pressure force should be written as $8\pi n_0 k(T_e + T_i)/B_0^2$. At $T_e = T_i$

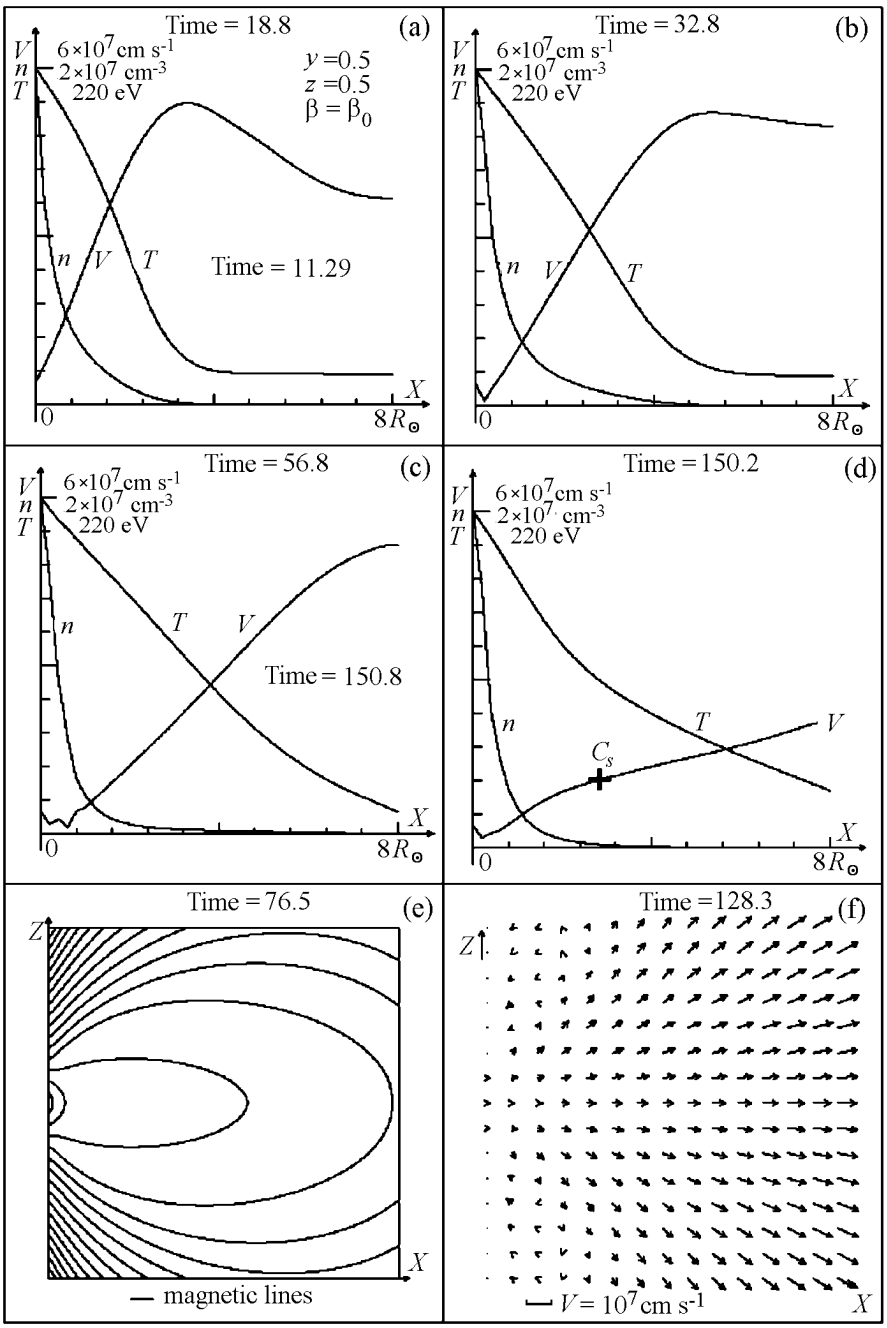

Figure 3. Results of calculations taking into account gravitation.

the dimensionless coefficient of pressure force in (3) should be taken to be $2\beta_0$ rather than β_0.

[19] To understand whether, in principle, the stationary outflow of solar wind can exist due to additional acceleration, we performed the calculations in which the pressure force was increased by a factor of 2, i.e., the dimensionless coefficient of pressure force in equation (3) was taken to be $2\beta_0$. The results of calculations are depicted in Figure 4. Figure 4a shows distributions of plasma parameters along the X axis for $t = 11.29$. The increases in plasma density and temperature occur here within the computational domain, and the velocity maximum has not yet reached the right boundary. The maximum velocity exceeds 5×10^7 cm s^{-1}. It is reached at the portion of the X axis where the pressure gradient is not zero. The magnetic field lines are extended at this portion by the flow of expanding plasma (Figure 4b). However, in the region nearer to the right boundary, where the plasma flow has not yet arrived, the field lines differ only slightly from the dipole ones. The velocity maximum shifts beyond the computational domain to the moment of

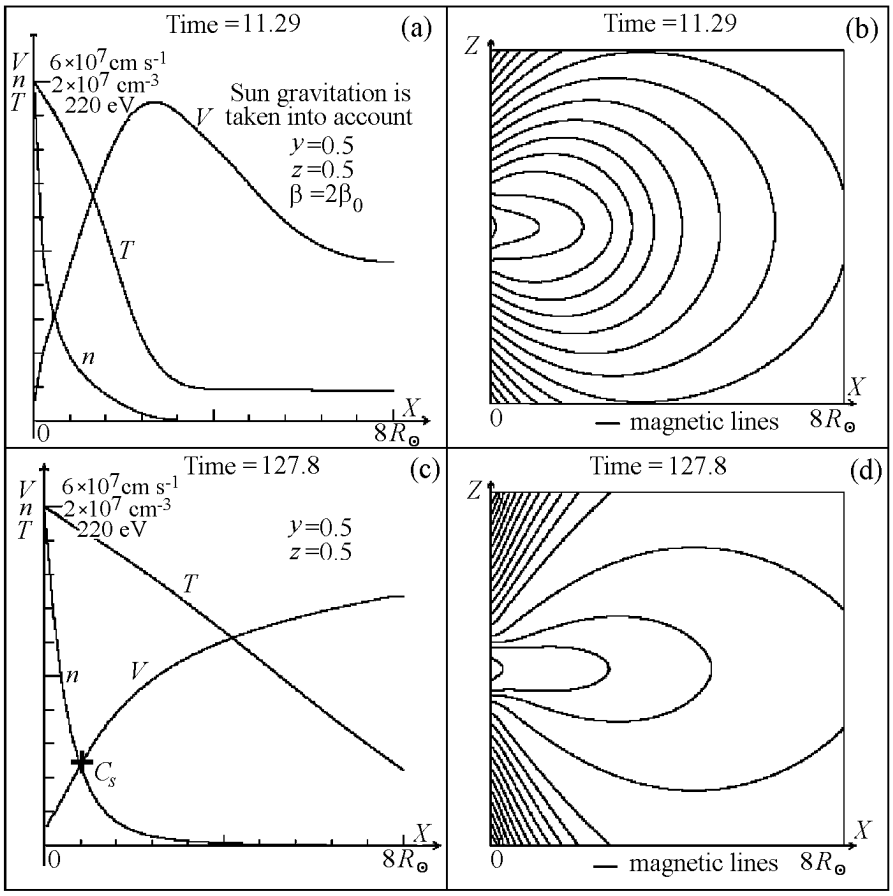

Figure 4. Results of calculations taking into account gravitation. The parameter β_0 is increased by a factor of 2.

time $t \sim 40$. Distributions of the plasma parameters and the field lines for $t = 127.29$, when the stationary flow is about to be established, are shown in Figures 4c and 4d. No local minima in velocity obtained in calculations ignoring ion temperature gradient (Figure 3) are observed near the left boundary. In this case acceleration by the pressure gradient is more effective, and influence of gravitation is not considerable. The cross marks the point of transition of the plasma flow to the supersonic regime. The transition occurs smoothly at a distance of $2.8\,R_\odot$ from the center of the Sun, while at neglecting ion pressure the distance of transition is $4.5\,R_\odot$. In both cases the magnetic field lines are extended in the entire computational domain, formation of the heliospheric current sheet in the computational domain takes place.

[20] Formation of the current sheet leads to turn of the magnetic field vectors. An increase of the radial component of the magnetic field near the sheet and a decrease of the transverse component in the sheet occur (Figures 5a and 5b). Distributions of the radial component of the magnetic field, plasma flow velocity, plasma density and current density across the sheet at a distance of 8 solar radii are shown in Figures 5c and 5d. These dependences have the regularities similar to those clearly observed at crossings of the current sheet by spacecrafts at large heliocentric distances. The current sheet is located inside a thicker layer with an increased plasma concentration, the minimum of the solar wind velocity is inside the sheet [*Borrini et al.*, 1981; *Smith*, 2001].

[21] Comparison of the results of calculations involving the coefficients of pressure force of β_0 and $2\beta_0$ shows that taking into account the ion temperature gradient provides the stationary thermal expansion of the solar corona plasma in the presence of gravitation and formation of the heliospheric current sheet. If this is so, introduction of the coefficient less than unity before the term in the equation of motion will lead to a change in the direction of velocity in the calculations including typical parameters of the corona and accretion of material. Figure 6 shows results of calculations for the coefficient equal to $(5/8)\beta_0$. Here, a local minimum of velocity arises near the left boundary already at $t \sim 20$, but the velocity is still directed away from the Sun, and the magnetic field lines are extended in this region. Later, the minimum becomes even deeper, and the velocity reverses the direction. The plasma flow from the corona changes the direction, and the plasma accumulates near the left boundary,

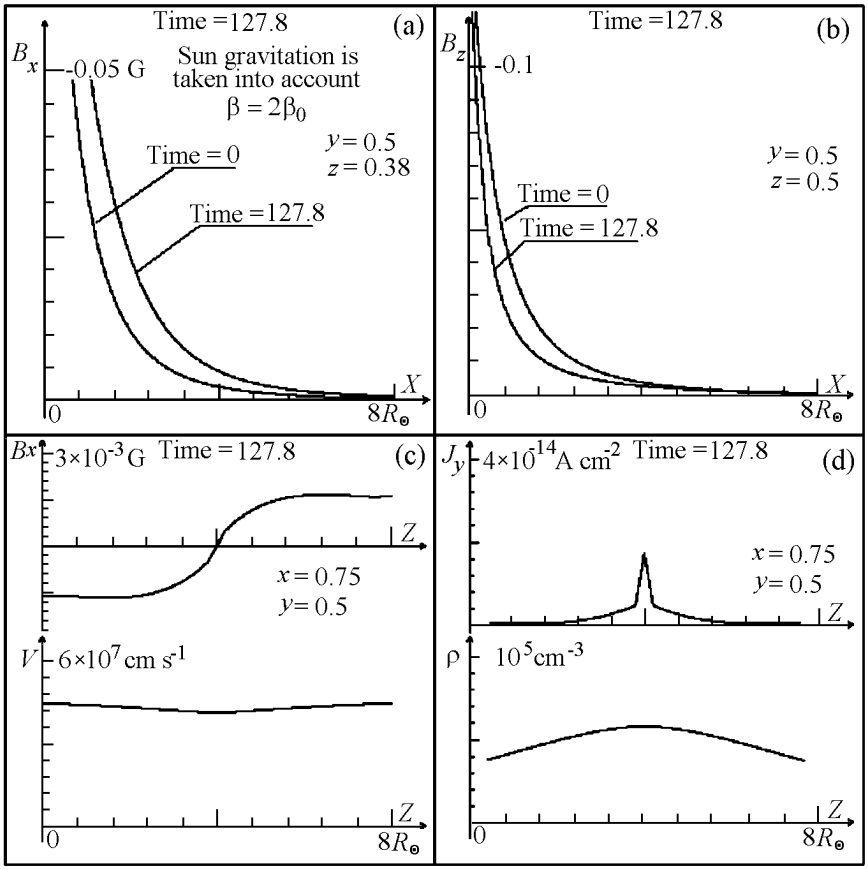

Figure 5. Radial distributions of (a and b) magnetic field components and (c and d) distributions of magnetic field, plasma velocity, and current and plasma densities.

where the boundary conditions are taken to be a constant corona density and plasma velocity corresponding to the loss of the solar mass. Thus, for the stable solar wind generation to take place, ions in the corona must be heated to the temperature close to the electron temperature.

5. Discussion

5.1. Estimation of the Heliospheric Current Sheet Thickness

[22] As a bounded conductor moves across the magnetic field, charges accumulate at its ends. In the steady state regime, current is zero. The electric field in the conductor is determined from the Ohm's law $\mathbf{E} + \mathbf{V} \times \mathbf{B}/c = j/\sigma$ by substituting $j = 0$. Another situation arises in the closed current of the heliospheric current sheet, i.e., no charge accumulation occurs, polarization field is absent, and the current density can be estimated as $j = \sigma \mathbf{V} B_\perp/c$. In an independent manner, the current density can be obtained from Ampere's equation rot$\mathbf{B} = 4\pi j/c$ or $j \approx cB/2\pi\delta$. By equating these expressions for j, we get the current sheet thickness $\delta = (c^2/2\pi\sigma V)(B/B_\perp)$. By substituting plasma parameters in the current sheet in the region of the Earth's orbit [*Smith*, 2001] – solar wind velocity in the current sheet $V \sim 3 \times 10^7$ cm s^{-1}, plasma concentration $n \sim 10$ cm^{-3}, magnetic field in the solar wind $B = 5\gamma$, Spitzer conductivity $\sigma = 10^{15}$ s^{-1} for $T_e = 20$ eV, and assuming the normal component of the magnetic field in the current sheet $B_\perp = 0.1\gamma$, we get $\delta \sim 2$ mm, which contradicts observations. The second contradiction is met in estimation of the current density from expression $j = \sigma V B_\perp/c$, where there are no limitations on the plasma density and velocity of charge carriers. The obtained value $j \sim 2 \times 10^6$ CGSE corresponds to the current velocity $V_C = j/n_e = 3 \times 10^{14}$ cm s^{-1}. The reason for the contradiction is the use of the Spitzer conductivity for the low-concentration plasma, when a high current density is not provided because of deficiency of charge carriers. Apparently, the maximum current velocity must not exceed the thermal velocity of electrons V_{th}, otherwise an anomalous resistance will develop. By taking the current velocity $V_{th} = 3 \times 10^8$ cm s^{-1}, we obtain the maxi-

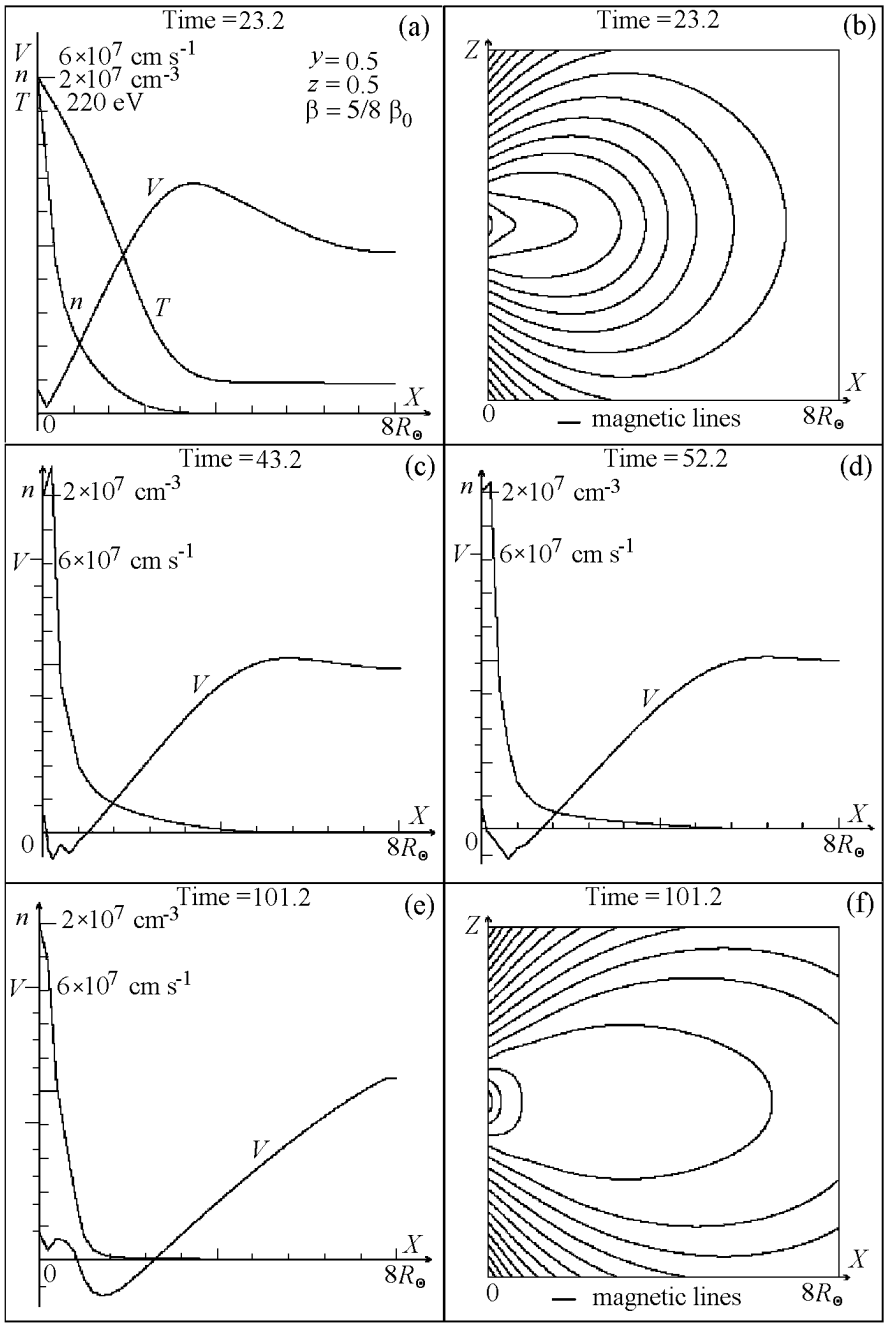

Figure 6. Results of calculations taking into account gravitation. The parameter β_0 is decreased by a factor of 1.6.

mum possible current density in the sheet of ∼1 CGSE, and the minimal possible thickness of the current sheet of about 2×10^5 cm. If the electron temperature is well above the ion one ($T_e > 3T_i$), the ion-sonic instability can develop already at $V_C \sim (T_e/M_i)^{1/2}$ [*Bernstein et al.*, 1960]. Then the maximum current density will become $(M_i/m_e)^{1/2}$ times lower, and the current sheet width can reach 2×10^7 cm. The sheet thickness estimated in such a manner is more than an order of magnitude lower than its maximum thickness (10,000 km) obtained from spacecraft measurements [*Smith*, 2001]. This can be explained by either a very low $B_\perp$ or development of current instability at $V_c \sim 0.1(T_e/M_i)^{1/2}$. In addition, the sheet thickness of 10,000 km is likely to be overestimated because the angle between the spacecraft trajectory and normal to the sheet surface at crossing of the heliospheric current sheet can be rather large.

5.2. Possibility of Reconnection in the Heliospheric Current Sheet

[23] Reconnection above the active corona region where $\beta \ll 1$ is an efficient mechanism of plasma heating. On the contrary, the reconnection in the solar wind cannot play a significant role in its energetics because at $\beta = 1$ the temperature increases only by a factor of two even in the case of total dissipation of the interplanetary field. As far as the heliospheric current sheet is concerned, the flow required for reconnection cannot be established. Indeed, reconnection occurs in the vicinity of the neutral X line at plasma inflow from both sides of the current sheet. After reconnection, the magnetic tension force accelerates the plasma along the sheet in both directions. However, motion of plasma toward the Sun is impossible in the heliospheric current sheet, because the sheet itself exists due to the flow directed away from the Sun. Thus the flow that must be established at reconnection is impossible in the heliospheric current sheet.

[24] The situation in the magnetospheric tail is different. The solar wind extends the magnetic field lines of the Earth. On the tail surface, the solar wind generates the current that closes in the current sheet. The current sheet of the tail plays the role of a load, while the heliospheric sheet is a generator. Inside the current sheet of the tail, the force accelerates plasma along the sheet rather than decelerates it. Earthward from the neutral X line, the force $\mathbf{j} \times \mathbf{B}/c$ and plasma flow are directed toward the Earth. On the other side from the X line, the normal component of the magnetic field has another direction, and plasma accelerates away from the Earth [*Lui*, 1987].

6. Conclusions

[25] Expansion of the solar corona and formation of the heliospheric current sheet have been studied in numerical experiment. To solve a complete system of three-dimensional MHD equations, the PERESVET code was used. The following have been shown:

[26] 1. At corona expansion, the solar magnetic field is extended by the plasma flow, and a current sheet is formed. The sheet is not neutral. It contains a normal component of the magnetic field.

[27] 2. The current generation in the current sheet is similar to the current generation in a short-circuited MHD generator.

[28] 3. Division of magnetic lines into closed and open is not reasonable.

[29] 4. At typical corona parameters and $T_i = T_e$, the inclusion of gravitation and electron and ion temperature gradients does not lead to disturbance of stability of the solar wind flow formed. If $T_i < T_e$, for the stable stationary flow to occur, an additional impulse, for instance, due to absorption of MHD disturbances propagating from the photosphere, is needed.

[30] 5. Transition from the subsonic flow to the supersonic one occurs at a distance of about $\sim 3R_\odot$. No discontinuities in parameters at transition to the supersonic flow are observed.

[31] **Acknowledgments.** The work was supported by the Russian Foundation for Basic Research, grant 01-02-16186 and Government Program "Astronomy."

References

Alfvén, H. (1981), *Cosmic Plasma,* Springer, New York.

Bernstein, I. B., E. A. Frieman, R. M. Kulsrud, and M. N. Rosenbluth (1960), Development of ion-sound instability, *Phys. Fluids, 3,* 136.

Borrini, G. J., T. Gosling, S. J. Bame, E. C. Feldman, and J. M. Wilcox (1981), Solar wind helium and hydrogen structure near the heliospheric current sheet: A signal of coronal streamers at 1 AU, *J. Geophys. Res., 86,* 4565.

Chashey, I. V. (1997), The role of MHD wave interaction in solar wind formation, *Astron. Z., 74,* 3.

Crooker, N. U., S. W. Kahler, J. T. Gosling, D. E. Larson, R. P. Lepping, E. J. Smith, and J. J. de Keyser (2001), Scales of heliospheric current sheet coherence between 1 and 5 AU, *J. Geophys. Res., 106,* 15,963.

Doschek, G. A., and U. Feldman (2000), Extreme-ultraviolet spectral line widths in quiet-sun coronal plasmas at distances of $1.03 \leq R_\odot \leq 1.45$ along the solar equatorial plane, *Astrophys. J., 529,* 599.

Israelevich, P. L., T. I. Gombosi, A. I. Ershkovich, K. C. Hansen, C. P. T. Groth, D. L. DeZeeuw, and K. G. Powell (2001), MHD simulation of the three-dimensional structure of the heliospheric current sheet, *Astron. Astrophys., 376,* 288.

Koutchmy, S., and M. Livshits (1992), Coronal streamers, *Space Sci. Rev., 61,* 393.

Laval, G., R. Pellat, and M. Vullemin (1966), Dynamics of the geomagnetic tail, in *Plasma Physics and Controlled Nuclear Fusion Research,* 2, p. 259, Int. Assoc. Energy Agency, Vienna, Austria.

Lui, A. T. Y. (1987), *Magnetotail Physics,* Johns Hopkins Univ. Press, Baltimore, Md.

Minami, S., M. Morimoto, A. I. Podgorny, and I. M. Podgorny (2002), Numerical simulation of a heliospheric current sheet creation due to coronal expansion, paper presented at 8th Asian-Pacific Regional Meeting, Int. Astron. Union, Tokyo, Japan.

Parker, E. N. (1963), *Interplanetary Dynamical Processes,* Interscience, Hoboken, N.J.

Pisanko, Yu. V. (1985), Calculation of stationary magnetohydrodynamic flows in formation of solar wind, *Geomagn. Aeron.* (in Russian), *25,* 17.

Pneuman, G. W., and R. A. Kopp (1971), Gas-magnetic field interactions in the solar corona, *Sol. Phys., 18,* 258.

Podgorny, A. I., and I. M. Podgorny (1995), Current sheet creation by super-Alfvénic jet in dipolar field, *Sol. Phys., 161,* 165.

Podgorny, A. I., and I. M. Podgorny (1996), Electrodynamical model of the flare and solar flare prognosis, *Astron. Soc. Pac. Conf. Ser., 95,* 66.

Podgorny, I. M., A. I. Podgorny, S. Minami, and M. Morimoto (2004), An MHD model for a Heliospheric Current Sheet, *Astronomy Report., 48,* 433.

Seely, J. F., U. Feldman, U. Schuhle, K. Wilhelm, W. Curdt, and P. Lemaire (1997), Turbulent velocities and ion temperatures in the solar corona obtained from SUMER line widths, *Astrophys. J., 484,* L87.

Smith, E. J. (2001), The heliospheric current sheet, *J. Geophys. Res., 106,* 15,819.

Somov, B. V., and S. I. Syrovatsky (1971), Current sheet formation on field drag by solar wind, *J. Exp. Theor. Phys.* (in Russian), *61,* 1864.

Usmanov, A. V. (1993), Interplanetary magnetic field structure and solar wind parameters as inferred from solar magnetic field observations and by using a numerical 2-D MHD model, *Sol. Phys., 143,* 345.

Usmanov, A. V. (1999), Magnetohydrodynamic models of solar wind, Dr. Sci. thesis, St. Petersburg University, St. Petersburg, Russia.

I. M. Podgorny, Institute of Astronomy, Russian Academy of Sciences, Moscow, Russia. (podgorny@inasan.ru)

A. I. Podgorny, P. N. Lebedev Physical Institute, Russian Academy of Sciences, Moscow, Russia.